

Effect of precursor on optical, dielectric properties of zirconia crystalline powder prepared by hydrothermal method

Rajababu Chintaparty*, N. Ramamanohar Reddy

Department of Materials Science and Nano technology, Yogi Vemana University, Kadapa 516003, India

*Corresponding author. E-mail: baburaja46@gmail.com

Received: 30 August 2015, Revised: 27 November 2015 and Accepted: 03 January 2016

ABSTRACT

Zirconium Oxide (zirconia) particles were prepared through hydrothermal technique by using zirconium oxychloride ($ZrOCl_2 \cdot 8H_2O$) and zirconyl nitrate ($ZrO(NO_3)_2 \cdot H_2O$) as precursors. The structural characterization as prepared samples were confirmed by X-ray powder diffraction (XRD) and showed monoclinic phase. Further, surface morphology of synthesized zirconia particles were confirmed by scanning electron microscopy (SEM). The energy band gap of synthesized samples was evaluated from UV-vis absorption spectra. The frequency dependence of dielectric constant and dielectric loss of the samples were investigated at room temperature. Zirconium oxychloride was found to be better precursor for obtaining ZrO_2 with a higher dielectric constant than Zirconyl nitrate under the same synthesis conditions. Copyright © 2016 VBRI Press.

Keywords: Hydrothermal method; monoclinic phase; dielectric; impedance analysis.

Introduction

Dielectric oxides play a very important role in microelectronics, optics and sensors for many years due to their unique properties such as high thermal stability, high dielectric constant, high refractive index, larger band gap, high ionic conductivity, etc. [1-4]. In recent years most of researchers focused on alternative material to silicon based dielectric devices for enhancement of storage density in dynamic random access memory, fabrication of very large scale integrated circuit, gate dielectrics, prevent chemical corrosion, oxidation in metals and to sense oxygen. In the view of above, zirconium Oxide (ZrO_2) is one of the promising candidate having its high dielectric constant, low toxicity, higher band gap and eco-friendly when compare to other ceramic oxides [5-13].

The properties of ZrO_2 based device strongly depends on phase and crystal size. It is, well known that; pure ZrO_2 exhibits three polymorphs namely cubic, tetragonal and monoclinic. The stable form at room temperature is the monoclinic phase, which is known to be transform to tetragonal phase at 1170 °C during heating, while this phase transform to cubic phase at 2370 °C [14,15]. Many physical and chemical methods have been adopted to prepare zirconium oxide, which include Atomic layer deposition, r.f magnetron sputtering / reactive sputtering, chemical vapour deposition, pulsed laser deposition, sol-gel dip coating/ spin coating, co-precipitation, hydrothermal method, etc.

In the above view, there were studies on effects of different environmental and synthetic conditions on the size, morphology and properties of zirconia particles through various methods [16-25]. However leading to change of precursor influence the optical and dielectric properties were rarely discussed. In the report we have

synthesized zirconia particles through hydrothermal method by using different precursors, we preferred hydrothermal technique as it is an ideal technique for synthesis of ceramic oxides with high purity, controlled stoichiometry, narrow particle size distribution, controlled morphology, microstructure and high crystallinity [26-29].

Experimental

Material

Zirconium oxychloride ($ZrOCl_2 \cdot 8H_2O$), zirconyl nitrate ($ZrO(NO_3)_2$), sodium hydroxide (NaOH) were purchased from analytic grade and used without further purification.

Synthesis of ZrO_2

Initially, 1M zirconium oxychloride and 4M sodium hydroxide aqueous solutions were prepared separately. In the next step NaOH solution was slowly added to zirconium oxychloride solution using hot plate magnetic stirrer to obtain homogeneous solution of pH value 12. This homogeneous solution was transferred in to an autoclave and is loaded in to an oven. The oven was maintained at 110 °C for 14 hours. After cooling to room temperature the autoclave was taken out from the oven. The precipitate was filtered, washed with distilled water and ethanol to reduce the agglomeration. The obtained powder was dried in an oven at 80 °C and then calcined at 1100 °C for 2 h. A similar procedure was carried out for preparation of zirconia particles using zirconyl nitrate as a precursor.

Characterization of synthesized materials

The phase analyses of the above prepared samples were characterized by X-ray diffraction (Model Rigaku ultima III). The surface morphology of prepared samples was

obtained by Scanning Electron Microscopy (JEOL JSM-6390 microscope). The optical properties were analyzed from UV-Vis spectrophotometer (Model: UV-3092). The dielectric properties were measured by low frequency impedance analyzer (Model HIOKI 3532-50).

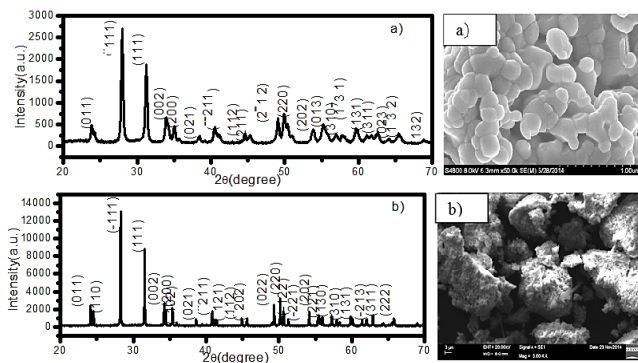


Fig. 1. XRD patterns and SEM images of zirconia particles prepared by hydrothermal method using different precursors: (a) $ZrOCl_2 \cdot 8H_2O$ (b) $ZrO(NO_3)_2 \cdot H_2O$.

Table 1. The calculated lattice parameters, unit cell volume, dislocation density and average crystallite size.

Sample	Precursor	Formula	Lattice parameters(A ^o)	Dislocation density ((lines/m ²) × 10 ¹³)	Average Crystallite size(nm)
1	Zirconium oxochloride	$ZrOCl_2 \cdot 8H_2O$	a=5.1142 b=5.2097 c=5.3112	1111.1	30
2	zirconyl nitrate	$ZrO(NO_3)_2 \cdot H_2O$	a=5.1450 b=5.2075 c=5.3107	7.3051	117

Results and discussion

Structural and microscopic studies

X-ray diffraction (XRD) patterns of synthesized samples were present in **Fig. 1**. From the **Fig. 1** it is observed that XRD patterns of all samples showed the characteristic peaks of their monoclinic phase of zirconia (JCPDS NO: 86-1449). Based on the X-ray diffraction data, we have calculated lattice parameters, unit cell volume, average crystallite size, dislocation density and number of unit cells and they were present **Table 1**. From the **Table 1** it can be seen that the estimated average crystallite size sample 1 was low when compared to sample 2 that could be reason for its high defect concentration and this leads large surface area and also evident that dislocation density was high for sample 1 compared to sample 2 that indicate that slow growth rate and high defects existing in crystallites [30, 31]. The morphology of the samples was obtained by SEM and they are as shown in **Fig. 1**. From the observation of **Fig. 1**, it is clear that the sample 1 particles are spherical shape, whereas sample 2 particles the formation of a continuous particulate network in the suspension structure. It is believed that differences in the nucleation process would have let to formation of varying ZrO_2 morphology. It is known that homogenous nucleation results in smaller size and uniform shape grains, While random nucleation results in larger size and irregular shape grains. In sample 1, homogenous nucleation seems to be taking place, while in other random nucleation was taken place[31].

Optical studies

Fig. 3 illustrates the UV absorption spectrum of synthesized samples was present in **Fig. 2**. From **Fig. 2**, it is

observed that the sample 1 showed around 229 nm, which could be arise due to transitions involving extrinsic states such as surface trap states or defect states or impurities, whereas sample 2 showed 290 nm. This peak was expected to transition from valence band to the conduction band [32]. It can be noted from the **Fig. 2** the absorbance is more prominent in the case of sample 2 because of the large size of the zirconia particles compared with sample 1 [33].

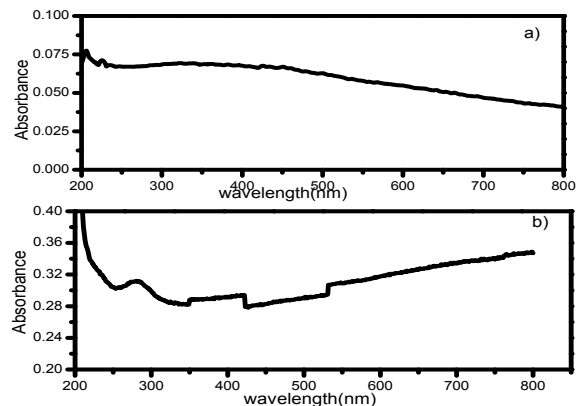


Fig. 2. UV-vis absorption spectra of (a) sample 1 and (b) sample 2.

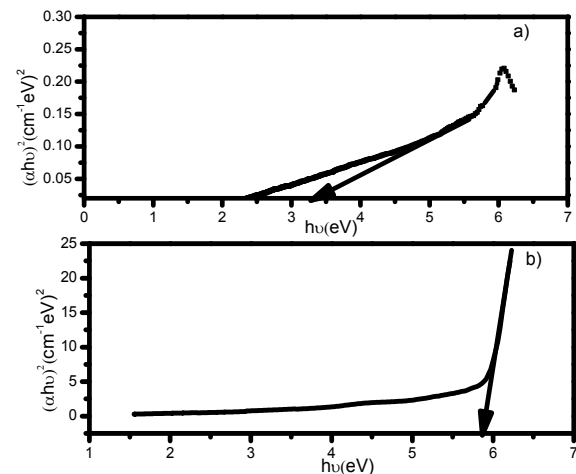


Fig. 3. $(\alpha h\nu)^2$ vs. $h\nu$ plots of (a) sample 1 and (b) sample 2.

A common way to estimate the band gap from optical absorption spectra is the Tauc plot, which is based on the assumption that energy dependent absorption coefficient can be expressed as [34]

$$\alpha = \frac{A(h\nu - E_g)^{\frac{n}{2}}}{h\nu} \quad (1)$$

where, A is proportionality constant, $h\nu$ is the photon energy and E_g is the band gap. The value of n is 1 for direct allowed transitions, 2 for non-metallic materials, 3 for forbidden transitions, 4 for indirect allowed transitions and 6 for indirect forbidden transitions. Now among the plot for $(\alpha h\nu)^2$, $(\alpha h\nu)$, $(\alpha h\nu)^{2/3}$, $(\alpha h\nu)^{1/2}$ and $(\alpha h\nu)^{1/3}$ as a function of photon energy $h\nu$, the best fitting was obtained with $n=1$ in **Eq (1)**, i.e. $(\alpha h\nu)^2$ as a function of $h\nu$ indicating that the band transition occurred are direct in nature.

The plot for $(\alpha h\nu)^2$ as function of $h\nu$ energy is shown in **Fig. 3** for the both sample 1 and sample 2. By extrapolating linear region of these curves to $(\alpha h\nu)^2=0$, the value of E_g of the sample 1 is found to be 3.4 eV while that of the sample 2 is estimated to be 5.8 eV [8, 32].

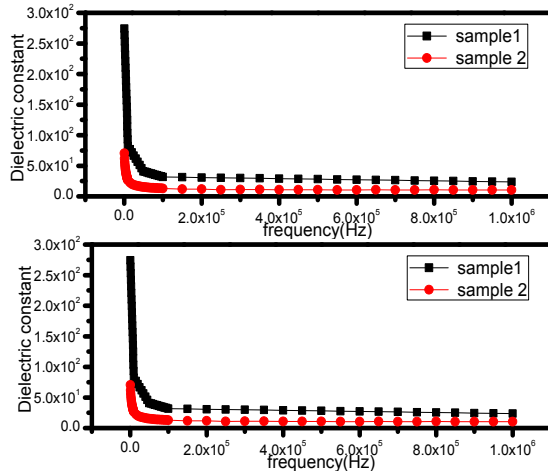


Fig. 4. Dielectric constant and loss as a function of frequency at different samples.

Dielectric studies

To carry out dielectric measurements, the powder samples were prepared in the form of circular disk shaped pellets and then pellets were sintered and polished by fine emery paper to make the surface smooth and parallel. The silver paste coating was applied on the opposite surface of pellets as an electrode with air drying conducting silver paste and also, there by forming parallel plate capacitor geometry to have a good ohmic contact.

The frequency variation of the capacitance and dielectric loss factor of prepared pellets were investigated at 1 KHz –1 MHz

The dielectric constant was calculated by using the formula

$$\epsilon' = \frac{C d}{\epsilon_0 A} \tag{2}$$

where, C is capacitance of pellet in pF, d is the thickness of pellet, A is the cross-sectional area of the flat surface of the pellet and ϵ_0 the permittivity for free space.

Complex impedance Z was calculated from the relation

$$Z = \frac{1}{i\omega C_0 \epsilon} \tag{3}$$

where, $C_0 = \frac{\epsilon_0 A}{d}$, is the geometrical capacitance and ω is the angular frequency.

Frequency dependence of dielectric constant for different crystallite sizes as shown in **Fig.4**. From **Fig. 4** it is observed that the dielectric constant decreases with increasing of frequency and attained almost constant value at higher frequency region. This is the common behaviour of ceramic oxides [35] and also observed that the crystallite size affects dielectric properties significantly. The dielectric constant of sample 1 is about two orders of magnitude compared to sample 2. It is well known that the decrease in

crystallite size increases the surface area and hence, dielectric constant is high [36]. Like dielectric constant, the dielectric loss also decreased with frequency for both samples as shown in **Fig. 4**. Observed high dielectric loss in the low frequency region may be due to a high defect charge density existing material [37].

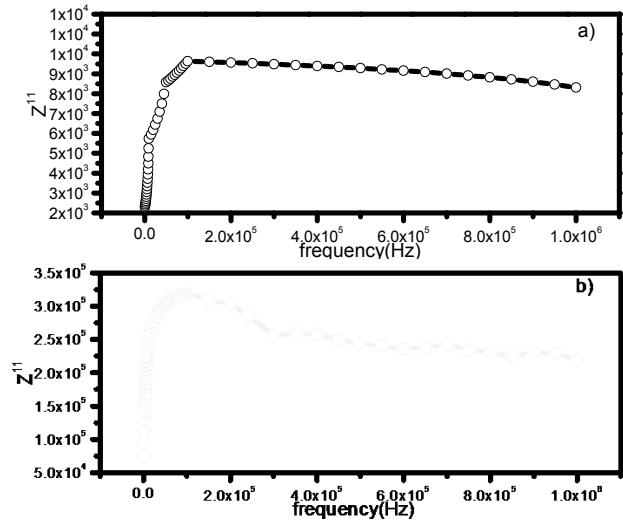


Fig. 5. Frequency versus Z^{11} of (a) sample 1 and (b) sample 2.

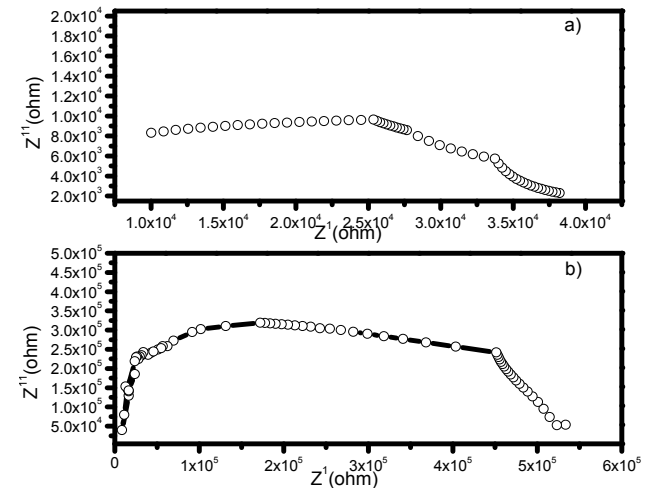


Fig. 6. Complex plane impedance plots of (a) sample 1 and (b) sample 2.

Synthesized zirconia particles show high dielectric constant at lower frequencies due to space charge polarization effects. It can be clearly understood through the impedance analysis as shown in **Fig. 5, 6**. **Fig. 5** shows the magnitude of imaginary impedance (Z^{11}) value increases as the frequency increases and finally merges in the high-frequency domain. This indicates the presence of space-charge polarization effects at lower frequency region [38, 39].

Fig. 6 shows the complex impedance (imaginary versus real) for the synthesized samples 1 and 2. The depression of the semicircle is considered further evidence of polarization phenomena with a distribution of relaxation times. The assignment of the two semicircular arcs to the electrical response is due to the grain interior and grain boundary which can be considered to be consistent with the brick-layer model for polycrystalline samples [40].

Conclusion

Synthesis of zirconia crystals were successfully performed by hydrothermal method using $ZrOCl_2 \cdot 8H_2O$ and $ZrO(NO_3)_2 \cdot H_2O$ as precursors. XRD study show that the synthesized ZrO_2 material is of pure monoclinic phase. The estimated average crystallite size of synthesized ZrO_2 using zirconium oxochloride as a precursor is low compared to zirconyl nitrate. The band gap was evaluated from UV-vis analysis. From these results we can say that minimum value obtained for zirconia particle using zirconium oxochloride as a precursor. The obtained dielectric constant values of synthesized zirconia were high using $ZrOCl_2 \cdot 8H_2O$ as a precursor compared to $ZrO(NO_3)_2 \cdot H_2O$.

Reference

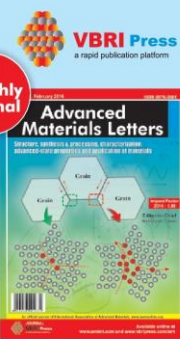
- Wilk, G. D.; Wallace, R. M.; Anthony, J. M., *Journal of Applied Physics*, **2011**, *10*, 5243.
DOI: [10.1063/1.136106](https://doi.org/10.1063/1.136106).
- G. M. Rignanese. X. Gone, *Physical review B*, **2004**, *69*,184301.
DOI: [10.1103/PhysRevB.69.184301](https://doi.org/10.1103/PhysRevB.69.184301)
- Kington, A.; Maria, J. P.; Streiffer, S. K., *Nature*, **2000**, *406*, 1032.
- Smith, D.; Snow, A.; Sible, L.; Ignont, E., *Journal of non-crystalline solids*, **2001**, *285*, 256.
DOI: [10.1016/S0022-3093\(01\)00464-1](https://doi.org/10.1016/S0022-3093(01)00464-1)
- Clarket, D. R.; Phillpot, Simon R.; *Materials Today*, **2005**, *8*, 22.
DOI: [10.1016/S1369-7021\(05\)70934-2](https://doi.org/10.1016/S1369-7021(05)70934-2)
- Lopez Ibanez, R.; Barrdo, J. R. R.; Martin, F.; Brucker, F.; Leinen, D., *Surface & Coatings Technology*, **2004**, *188*, 675.
DOI: [10.1016/j.surfcoat.2004.07.002](https://doi.org/10.1016/j.surfcoat.2004.07.002)
- Spirig, John V.; Ramamoorthy, Akbar, S. A.; Routbort, J. L.; Singh, D.; Dutta, P. K., *Sensors and Actuators B*, **2007**, *124*,192.
DOI: [10.1016/j.snb.2006.12.022](https://doi.org/10.1016/j.snb.2006.12.022)
- Taguchi, M.; Takayuki, N.; Akiyuki, M.; Yoshio, S.; Tetsuo, U.; Toshihata, F.; Takashi, N., *Journal of super critical fluids*, **2014**, *85*, 57.
DOI: [10.1016/j.supflu.2013.11.001](https://doi.org/10.1016/j.supflu.2013.11.001)
- Padmamalini, N.; Ambujam, K.; *J. superlattice and microstructures*, **2014**, *76*, 376.
DOI: [10.1016/j.spmi.2014.10.021](https://doi.org/10.1016/j.spmi.2014.10.021)
- Chun, Z.; Ce Zhou, Z.; Matthew, W.; Taylor, S.; Paul, C., *Nano review*, **2013**, *1*, 456.
DOI: [10.1186/1556-276X-8-456](https://doi.org/10.1186/1556-276X-8-456)
- Sung, H. T.; Rucel, D.; Bo-Rucel, C.; Jyh-Shiarn, C., *J. Applied Physics*, **2014**, *54*, 1.
DOI: [10.7567/JJAP.54.01AD01](https://doi.org/10.7567/JJAP.54.01AD01)
- Debashis, P.; Tseung-Yuen, T., *Thin solid Films*, **2013**, *1*, 531.
DOI: [10.1016/j.tsf.2013.01.004](https://doi.org/10.1016/j.tsf.2013.01.004)
- Cooper, D.; Gollidge, G.; Zinc and zirconia, *Journal of RSC.*, London, 25.
- Barnard, A. S.; Yeredla, R. R.; Xu, H.; *Nanotechnology*, **2006**, *17*, 3039.
DOI: [10.1088/0957-4484/17/12/038](https://doi.org/10.1088/0957-4484/17/12/038)
- Kumari, L.; Li, W.; Wang, D., *Nanotechnology*, **2008**, *19*, 195602.
DOI: [10.1088/0957-4484/19/19/195602](https://doi.org/10.1088/0957-4484/19/19/195602)
- Kumar, M.; Reddy, G. B., *Materials Research Society*, **2008**, 1074.
DOI: [10.1557/PROC-1074-I10-34](https://doi.org/10.1557/PROC-1074-I10-34)
- Amor, S. Ben.; Rogier, B.; Baud, G.; Jacquet, M.; Nardin, M., *Materials Science and Engineering B*, **1998**, *57*, 28.
DOI: [10.1016/S0921-5107\(98\)00205-0](https://doi.org/10.1016/S0921-5107(98)00205-0)
- Soyez, G.; Eastman, J. A.; Thompson, L. J.; Bai, G. R.; Baldo, P. M.; McCormick, A. W., *Applied Physics letters*, **2000**, *77*, 1155.
DOI: [10.1063/1.1289803](https://doi.org/10.1063/1.1289803)
- Ehrhart, G.; Capoen, B.; Robbe, O.; Beclin, F.; Boy, Ph.; Turrell S.; Bouazaoui, M., *Optical Materials*, **2008**, *30*,155.
DOI: [10.1016/j.optmat.2007.10.004](https://doi.org/10.1016/j.optmat.2007.10.004)
- Kumari, L.; Li, W. Z.; Xu, J. M.; Leblanc, R. M.; Yili, D. Z. Wang.; Guo, H. H.; Zhang J., *Crystal Growth & Design*, **2009**, *9*, 3874.
DOI: [10.1021/cg800711m](https://doi.org/10.1021/cg800711m)
- Beena, T.; Kalpesh, S.; Basha, S.; Raksh, V., *Materials and interfaces*, **2006**, *45*, 8643.
DOI: [10.1021/ie060519p](https://doi.org/10.1021/ie060519p)
- Piticescu, R. R.; Monty, C.; Taloi, D.; Motoc, A.; Axinte, S., *Journal of the European Ceramic Society*, **2001**, *21*, 2057.
DOI: [10.1016/S0955-2219\(01\)00171-6](https://doi.org/10.1016/S0955-2219(01)00171-6)
- Becker, J.; Hald, P.; Bremholm, M.; Pedersen, J. S.; Chevallier, J.; Iversen, S. B.; Iversen, B. B., *ACS Nano*, **2008**, 1058.
DOI: [10.1021/nm7002426](https://doi.org/10.1021/nm7002426)
- Hakuta, Y.; Ohashi, T.; Hayashi, H.; Arai, K., *Journal of Materials Research*, **2004**, *19*, 2230.
DOI: [10.1557/JMR.2004.0314](https://doi.org/10.1557/JMR.2004.0314)
- Liu1, X. L.; Zhang, Q.; Chen, G. X.; Li, D.; Yang, B., *Materials Research Innovations*, **2013**, *7*, 478.
DOI: [10.1179/1433075X13Y.0000000096](https://doi.org/10.1179/1433075X13Y.0000000096)
- Kumari, L.; Du, G. H.; Li, W. Z.; Vennila, R. Selva.; Saxena, S. K.; Wang, D. Z., *Ceramics International*, **2009**, *35*, 2401.
DOI: [10.1016/j.ceramint.2009.02.007](https://doi.org/10.1016/j.ceramint.2009.02.007)
- Byrappa, K.; Adschiri, T., *Progress in Crystal Growth and Characterization of Materials*, **2007**, *53*,117.
DOI: [10.1016/j.pcrysgrow.2007.04.001](https://doi.org/10.1016/j.pcrysgrow.2007.04.001).
- Robert Piticescu, Claude Monty, Donats Millers, *Sensors and actuators*, **2005**, 102.
DOI: [10.1016/j.snb.2005.03.092](https://doi.org/10.1016/j.snb.2005.03.092)
- Weidong S.; Shuyan Song, Hongjie Zhang, *Chem Soc Rev*, **2013**, *42*, 5714.
DOI: [10.1039/c3cs60012b](https://doi.org/10.1039/c3cs60012b)
- Minori, T.; Seiichi, T.; Tadafumi, A.; Takayuki, N.; Koichi, S.; Takashi, N., *Cryst Eng Comm*, **2012**, *14*, 2117.
DOI: [10.1039/c2ce06408a](https://doi.org/10.1039/c2ce06408a)
- Marcelstoia, S.; Paul, B.; Lucianbarbu, T.; Adina, N.; Floricica, B. *J. Crystal Growth*, **2013**, *381*, 93.
DOI: [10.1016/j.jcrysgro.2013.07.018](https://doi.org/10.1016/j.jcrysgro.2013.07.018).
- Fatemeh, D.; Mahammad Reza, L. E., *Ceramics International* **2014**, *40*, 8427.
DOI: [10.1016/j.ceramint.2014.01.052](https://doi.org/10.1016/j.ceramint.2014.01.052).
- Kumar, M.; Suchand sandeep C. S.; Kumar, G.; Mishra, Y. K.; Philip, R.; Reddy, G. B., **2013**.
DOI: [10.1007/s11468-013-9605-z](https://doi.org/10.1007/s11468-013-9605-z).
- Dutta, S.; Som, S.; Priya, J.; Sharama, S. K. *Solid State Science* **2013**, *18*, 114.
DOI: [10.1016/j.solidstatesciences.2013.01.012](https://doi.org/10.1016/j.solidstatesciences.2013.01.012)
- Alias, R., *InTech*, **2013**, 90.
DOI: [10.5772/54037](https://doi.org/10.5772/54037).
- Sujit, M.; Ghosal T.; De, S. K., *J. Phys. D: Appl. Phys.*, **2010**, *43*, 1.
DOI: [10.1088/0022-3727/43/29/295403](https://doi.org/10.1088/0022-3727/43/29/295403).
- Pazhani, R.; Padma Kumar, H.; Angeo Varghese, A. Mose Ezhil Raj, Sam Solomon, Thomas. J. K., *Journal of alloys and compounds*, **2011**, *509*, 6819.
DOI: [10.1016/j.jallcom.2011.03.089](https://doi.org/10.1016/j.jallcom.2011.03.089).
- Chandra Babu, B.; Naveen Kumar, K.; Rudramadevi, B. H., *Ferroelectric letters.*, **2014**, *41*, 28.
DOI: [10.1080/07315171.2014.908682](https://doi.org/10.1080/07315171.2014.908682).
- Nayaka, P.; Badapandab, T.; Anwar, S.; Panigrahi, S., *phase transition*, **2015**, 1.
DOI: [10.1080/01411594.2014.987674](https://doi.org/10.1080/01411594.2014.987674).
- Rajababu, C.; Ramamanohar Reddy N. Kishore Reddy, I., *Ceramic International*, **2015**, 10675.
DOI: [10.1016/j.ceramint.2015.04.168](https://doi.org/10.1016/j.ceramint.2015.04.168)

Advanced Materials Letters

Copyright © 2016 VBRI Press AB, Sweden
www.vbripress.com/aml

Publish your article in this journal

Advanced Materials Letters is an official international journal of International Association of Advanced Materials (IAAM, www.iaamonline.org) published monthly by VBRI Press AB from Sweden. The journal is intended to provide high-quality peer-review articles in the fascinating field of materials science and technology particularly in the area of structure, synthesis and processing, characterisation, advanced-state properties and applications of materials. All published articles are indexed in various databases and are available download for free. The manuscript management system is completely electronic and has fast and fair peer-review process. The journal includes review article, research article, notes, letter to editor and short communications.



VBRI Press

a rapid publication platform

A Monthly Journal